

Observing Ocean Surface Waves with GPS-Tracked Buoys

T. H. C. HERBERS AND P. F. JESSEN

Department of Oceanography, Naval Postgraduate School, Monterey, California

T. T. JANSSEN

Department of Geosciences, San Francisco State University, San Francisco, California

D. B. COLBERT AND J. H. MACMAHAN

Department of Oceanography, Naval Postgraduate School, Monterey, California

(Manuscript received 8 August 2011, in final form 2 February 2012)

ABSTRACT

Surface-following buoys are widely used to collect routine ocean wave measurements. While accelerometer and tilt sensors have been used for decades to measure the wave-induced buoy displacements, alternative global positioning system (GPS) sensor packages have been introduced recently that are generally smaller, less expensive, and do not require calibration. In this study, the capabilities of several GPS sensors are evaluated with field observations in wind-sea and swell conditions off the California coast. The GPS buoys used in this study include Datawell Directional Waverider and Mini Directional Waverider buoys equipped with a specialized GPS Doppler shift sensor, and a low-cost experimental drifter equipped with an “off the shelf” GPS receiver for absolute position tracking. Various GPS position receivers were attached to the Waverider buoys to evaluate their potential use in low-cost wave-resolving drifters. Intercomparisons between the Datawell GPS-based buoys, the experimental GPS drifter, and a conventional Datawell buoy with an accelerometer–tilt–compass sensor package, show good agreement in estimates of wave frequency and direction spectra. Despite the limited (several meters) absolute accuracy of the GPS position receivers, the horizontal wave orbital displacements are accurately resolved, even in benign (significant wave height less than 1 m) swell conditions. Vertical sea surface displacements were not well resolved by the GPS position receivers with built-in or small patch antennas, but accurately measured when an external precision antenna was attached to the drifter. Overall, the field tests show excellent agreement between Datawell buoys using GPS and motion-sensor packages, and demonstrate the feasibility of observing ocean surface waves with low-cost GPS-tracked drifters.

1. Introduction

Surface-following buoys are widely used to collect in situ measurements of ocean surface waves. Early examples of these so called “pitch/roll buoys” were equipped with heave–pitch–roll sensors, and a compass to measure the sea surface height and slopes from which wave frequency spectra and (parameterized) directional spectra can be extracted (e.g., Longuet-Higgins et al. 1963; Mitsuyasu et al. 1975; Long 1980). The pitch/roll sensors were subsequently augmented with fixed accelerometers

to measure horizontal wave orbital displacements that provide more robust wave direction estimates than surface slopes. Intercomparisons of a variety of pitch/roll buoys have demonstrated their utility for reliable routine wave measurements (e.g., Allender et al. 1989; Barstow et al. 1991; Anctil et al. 1993; O’Reilly et al. 1996).

More recently, alternative sensor packages have been introduced based on the global positioning system (GPS; Hauser et al. 2005). An early version of these GPS buoys, the Seatex Smart-800 buoy used differential measurements of the Doppler shift in GPS signals to determine the horizontal and vertical velocities of the buoy (Krogstad et al. 1999). The Datawell DWR-G buoy also uses GPS velocity measurements but based on a single GPS receiver, thus eliminating the need for an additional shore station to provide differential corrections (de Vries et al. 2003).

Corresponding author address: Dr. Thomas H. C. Herbers, Department of Oceanography, Naval Postgraduate School, Monterey, CA 93943.
E-mail: thherber@nps.edu

A GPS buoy has several advantages. First of all, there are no mechanical moving parts that require delicate handling and maintenance. Second, the buoy velocities are determined directly in a fixed reference frame from external GPS signals, thus eliminating the need for calibration of an onboard motion-sensor package and compass. The use of a GPS receiver, as opposed to an autonomous instrument package, reduces the cost and enables the development of smaller buoys (e.g., the 40-cm diameter Datawell DWR-G4) that can be easily deployed by hand from a small vessel. A possible drawback of the GPS measurement approach is that it relies on a satellite link, which may be interrupted (e.g., when the buoy is submerged in breaking waves), resulting in occasional drop-outs in the wave records.

GPS technology has also been adopted in the development of drifters that track ocean surface currents. George and Largier (1996) introduced a GPS-tracked drifter for coastal and estuarine applications. Schmidt et al. (2003) developed a similar instrument for surf zone applications. Both these drifters utilized a differential GPS system to track the position of the drifters relative to a base station on shore to achieve the high accuracy (errors less than 5 m) needed to resolve the finescale structure of near shore flows.

Whereas for high-accuracy applications (e.g., surveying) differential GPS systems are needed, the removal of the “selective availability” of GPS signals for civilian application in 2000 has greatly improved the accuracy of non-differential GPS systems, which are much less expensive and do not require a base station. Johnson et al. (2003) developed a nondifferential GPS drifter for nearshore applications that can be deployed in large numbers at relatively low cost. MacMahan et al. (2009) developed a similar low-cost GPS drifter system for surf-zone applications, which takes advantage of recent developments in compact internal-logging GPS receivers that incorporate real-time differential corrections from a network of base stations through the Satellite-Based Augmentation System (SBAS). The real-time position accuracy of drifters using these “off the shelf” GPS receivers is about 2–3 m and can be improved to submeter accuracy with postprocessing techniques (MacMahan et al. 2009).

Whereas these recent drifter studies focused on measuring mean currents, the potential for resolving fluctuating orbital motion of surface waves in GPS position data has received less attention. Although the 2–3-m absolute accuracy of SBAS-enabled GPS receivers is very coarse compared with typical wave orbital displacements, the ability to resolve motions in the wind-wave and swell frequency band (nominally 0.05–0.5 Hz) is determined by the dynamic response characteristics of GPS signals at these frequencies, which are not well understood.

In this study, the wave-resolving capabilities of several off-the-shelf SBAS-enabled GPS receivers are examined, to explore their potential use in a low-cost drifter that measures both waves and currents. The receivers were attached externally to Datawell Waverider buoys, and continuous records of the vertical and horizontal buoy displacements were collected independently with both the Datawell sensor package and the GPS receiver to allow for quantitative comparisons. Multiple buoys, including both the newer GPS-based buoys and mini-buoys, and the traditional accelerometer-based buoys, were deployed in deep water off the California coast in a range of wind-sea and swell conditions. Additionally, a few low-cost experimental wave-resolving GPS drifters were evaluated by deploying them alongside drifting Datawell buoys. The field experiment and data collection are described in section 2, followed by analysis procedures in section 3. Intercomparisons of wave measurements from different sensors on the same buoy are presented in section 4. The performance of the experimental GPS drifters is evaluated in section 5 by comparing estimates of wave frequency and direction spectra with those obtained from the nearby Datawell buoys. The results are summarized in section 6.

2. Experiment

A field evaluation of GPS-based ocean wave measurements, using a variety of buoys and GPS sensors, was conducted in deep water off the California coast (Fig. 1) as part of the Office of Naval Research High-Resolution Air–Sea Interaction (HIRES) research initiative. The first set of field data were collected in a week-long pilot experiment in June 2009 offshore of San Clemente Island located on the seaward side of the Southern California Bight. This site provided a benign wave environment dominated by long-period swell from the Southern Hemisphere. The pilot experiment was followed by a month-long main experiment in June 2010 off the northern California coast near Bodega Bay. The latter site was chosen to capture the energetic wind-sea conditions driven by persistent strong alongshore winds.

In both experiments, drifting surface-following wave buoys were deployed on numerous occasions to provide in situ wave measurements for air–sea interaction studies conducted with ship-board and airborne sensors, and (in 2010) from the deep water floating platform FLIP. The buoys (described in more detail below) include three different types of Datawell Directional Waverider buoys as well as a prototype lower-cost drifter equipped with an off-the-shelf GPS position receiver. Several different models of GPS position receivers were attached to the Datawell

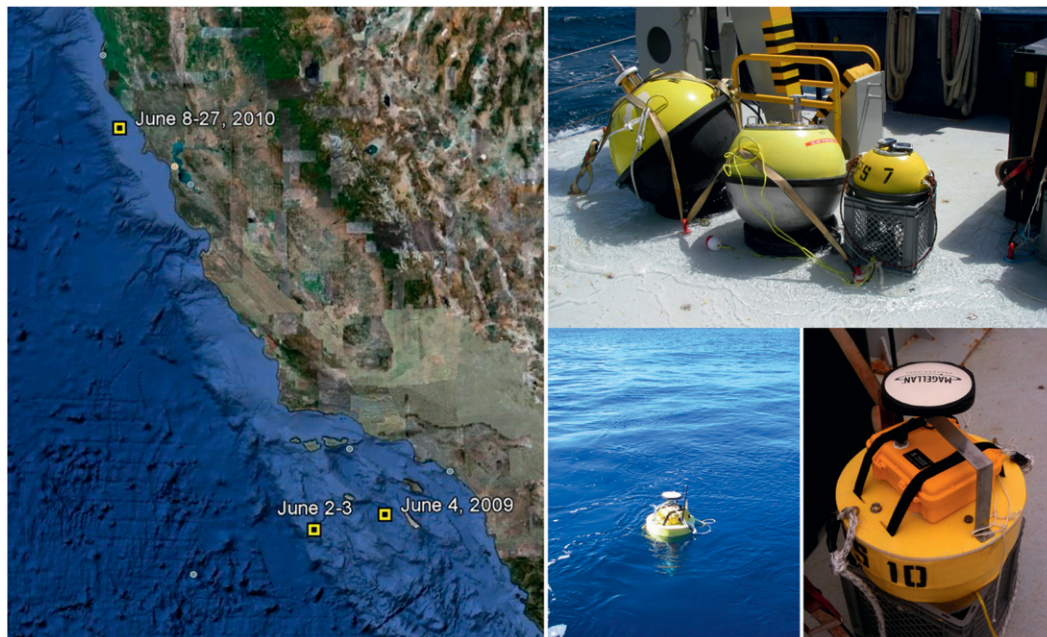


FIG. 1. Field site and instrumentation. (left) The locations of the buoy deployments off the Southern California coast in 2009 and the northern California coast in 2010. (top right, from left to right) Datawell DWR Mk-II, DWR-G7, and DWR-G4 buoys. (bottom) A prototype GPS drifter in the ocean and up close. The Pelican case holds the Magellan Mobile Mapper CX GPS receiver and an RF transmitter. The Ashtech ProMark3 NAP100 antenna is mounted on the handlebar.

buoys to evaluate their potential use as low-cost sensors in wave-resolving drifters.

a. *Waverider buoys*

The fleet of Datawell Directional Waverider buoys used in the experiment includes two DWR Mk-II, two DWR-G7, and three DWR-G4 buoys (Table 1 and Fig. 1).

The 90-cm-diameter DWR Mk-II buoys use a traditional motion-sensor package consisting of three-component accelerometers–tilt–compass sensors. These buoys have been widely used for decades and their accuracy and reliability are well established (e.g., O’Reilly et al. 1996). The internal processor in the buoy applies a double integration to the acceleration time series and (using the

compass and tilt measurements) produces three-component displacements in a fixed north–west–vertical coordinate frame.

The newer DWR-G buoys use a specialized GPS sensor package that measures the horizontal and vertical buoy velocities based on the Doppler shift in received GPS signals. These velocities are integrated internally in the buoy to produce north–west–vertical displacement time series, equivalent to the data stream recorded by the accelerometer-based buoy. The DWR-G7 buoy is a 70-cm-diameter buoy designed for long-term moored deployments, whereas the DWR-G4 is a smaller, 40-cm-diameter minibuoy for shorter duration drifting deployments.

TABLE 1. Overview of surface following buoys used in this study.

Buoy model	Internal buoy sensor package	External GPS position receiver(s)	No. of buoys
Datawell DWR Mk-II (90-cm diameter)	Accelerometers–tilt–compass sensors	Magellan MobileMapper CX with Ashtech ProMark 3 NAP100 antenna and Locosys Genie GT-31	2
Datawell DWR-G7 (70-cm diameter)	GPS Doppler shift sensor	Locosys Genie GT-31 (2) (drifting) or GlobalSat MR-350 (moored)	2
Datawell DWR-G4 (40-cm diameter)	GPS Doppler shift sensor	Locosys Genie GT-31 (2)	3
Prototype drifter (45-cm diameter)		Magellan MobileMapper CX with Ashtech ProMark 3 NAP100 antenna	2

A first field test of the DWR-G buoy was reported by de Vries et al. (2003) who mounted the GPS sensor package on a traditional accelerometer-based Datawell buoy to facilitate sensor intercomparisons. Excellent agreement between the accelerometer-based buoy measurements and those obtained with the DWR-G sensor on the same buoy for a range of swell conditions confirmed the high accuracy of the new GPS-based wave measurements. Few other field studies of DWR-G buoys have been reported so far, and an objective of the present study was to evaluate the performance of DWR-G buoys in a range of sea states, especially high wind conditions with steep breaking waves that may affect the quality of the GPS signal reception.

All Datawell buoys output a standard data stream consisting of continuous north–west–vertical displacement time series sampled at 1.28 Hz and processed frequency and directional moment spectra, together with various bulk wave parameters. The DWR-G buoy data were recorded with an internal datalogger while the DWR Mk-II buoy data were transmitted via a radio link to receivers on the supporting research vessel R/V *Gordon Sproul* where the data were archived during the cruises.

During the 2009 and 2010 experiments, numerous short-term buoy deployments were conducted during which a subset of the Datawell buoys was drifting freely for 2–6 h in the footprint of various radar and lidar remote sensing systems. In the 2010 main experiment, one of the DWR-G7 buoys was moored in 157-m depth near the Floating Instrument Platform (FLIP) to provide continuous wave measurements.

b. GPS receivers

One or more self-contained, internal logging GPS receivers were attached to each Datawell buoy to record the drift track and to investigate the feasibility of collecting wave measurements with relatively inexpensive GPS sensors. The larger DWR Mk-II buoys were equipped with a Magellan Mobile Mapper CX and a precision Ashtech ProMark3 NAP100 antenna to enhance the GPS signal reception. This receiver (and others discussed below) was operated in standard SBAS mode, incorporating real-time differential corrections from the North America Wide Angle Augmentation System (WAAS). The external antenna was chosen (instead of a simple patch antenna) after initial field tests in Monterey Bay showed that it improved dramatically the quality of vertical elevation measurements.

The Magellan system requires an approximately 0.4-m-diameter platform to support the waterproof housing of the receiver and the external antenna. A more compact system is the Locosys Genie GT-31, a self-contained GPS receiver with internal datalogger and antenna in a small (about the size of a cell phone) waterproof

housing that can be attached to almost any size surface float. The receiver contains the widely used SIRF Star III low power chip for up to 20-channel SBAS data processing. One or more of the Locosys units was attached to each of the drifting Datawell buoys to track the buoy position and evaluate the potential wave-resolving capability of the GPS receiver. This inexpensive (less than \$200 per unit) GPS receiver may be an attractive sensor for use in compact, low-cost drifters, deployed in large numbers to observe the spatial variability of nearshore currents and waves (e.g., Johnson et al. 2003; MacMahan et al. 2009).

A third GPS system used in the present study is the GlobalSat MR-350 that contains the same chip set as the Locosys units, but instead of an integrated system it is a stand-alone bulkhead antenna–receiver for use with an external data acquisition system. It was interfaced with an external datalogger and power supply to allow for longer-term (up to 5 days) GPS data collection on one of the Datawell DWR-G7 buoys that was moored near FLIP during the 2010 deployment.

All GPS systems were configured to record three-component (north–west–vertical) position data continuously with a sample rate of 1 Hz. The Magellan and GlobalSat receivers were augmented with radio transmitters to allow for real-time buoy position tracking from a nearby vessel.

c. Experimental GPS drifters

In addition to the Datawell buoys, a few prototype wave-resolving GPS drifters were fabricated for the 2010 main experiment. The objective of this initial field test was to assess the feasibility of collecting reliable wave measurements with a compact, low-cost (about \$4,000 for a complete system) drifting buoy that can be deployed easily by hand from a small boat. The drifter (Fig. 1, bottom panels) consists of three Polyethylene closed cell foam discs sandwiched between two Delrin plates. Each foam disc is 10 cm thick with diameters 45 (top), 40 (middle), and 35 (bottom) cm. A Magellan Mobile Mapper CX GPS receiver, spare battery pack, and an RF transmitter, are housed in a waterproof Pelican case. The Ashtech ProMark3 NAP100 antenna is supported by a metal handle bar (Fig. 1, bottom-right panel). About 25 pounds of ballast chain is attached to the bottom plate, giving the buoy a draft of about 25 cm, thus providing a stable platform for the GPS sensor package (Fig. 1, bottom-middle panel). Two identical drifters were deployed alongside the Datawell buoys to facilitate detailed intercomparisons of the observed wave statistics.

3. Data analysis

Drifting buoy deployments were conducted every day from 2 to 6 June 2009 and on selected days from 5 to

TABLE 2. Overview of case studies selected for analysis.

Date	Start time (UTC)	Buoys			Prototype drifter	Significant wave height (m)
		Datawell DWR Mark-II	Datawell DWR-G7	Datawell DWR-G4		
2 Jun 2009	2000	1	1	2		1.02
3 Jun 2009	1830	1	2	2		0.89
4 Jun 2009	1830	1	2	2		0.83
8 Jun 2010	0300		1 (Moored)			2.54
8 Jun 2010	2300		1 (Moored)	2		1.52
11 Jun 2010	1520		1 (Moored)			3.14
12 Jun 2010	2320		1	2	1	1.71
14 Jun 2010	1350		1 (Moored)			3.98
18 Jun 2010	0900		1 (Moored)			2.95
21 Jun 2010	2000		1 (Moored)	1	2	2.04
25 Jun 2010	2050		2	1	1	1.74
27 Jun 2010	1930			1	2	2.14

25 June 2010. These deployments varied in length from less than 2 h to about 6 h. To apply a consistent spectral analysis to the data, a common record length of 8192 s was chosen for each of the case studies. This relatively long record length (cf. the 20–30-min records usually used in routine wave monitoring applications) was chosen to reduce as much as possible any sampling variability in the spectral estimates that may obscure the identification of distinct spectral peaks and (when comparing spatially separated buoys) differences in the performance of different buoys and sensors. The prevailing conditions at the two field sites of remotely generated swell (2009) and developed wind seas driven by persistent strong along-shore winds (2010) have time scales of variation that are longer (typically 6–12 h) than several hours, and thus permit the analysis of 2-h-long records with relatively steady wave conditions.

No drifting buoys were deployed during the most energetic wave events in the 2010 experiment, but a moored DWR-G7 buoy was operational during these events and a few records from this buoy were included in the analysis to span a wide range of sea states with significant wave heights varying from 0.8 to 4.0 m (Table 2).

a. Data screening

For each of the drifting buoy deployments a record was chosen with relatively steady wave conditions. Nonsteady wave conditions do not necessarily invalidate the intercomparisons of different sensors and buoys (i.e., the instruments experience the same temporal evolution of wave statistics), but increase the sampling variability and complicate the interpretation of the wave spectra. To exclude evolving wave fields from the analysis a crude criterion was applied requiring significant wave height variations (estimated from 10-min-long data segments) to remain within the expected roughly $\pm 10\%$ sampling variability over the

selected record. Cases with larger wave height variations, or that did not contain a long enough wave record, were excluded from the analysis. Also excluded were drifter deployments where the buoys were more than 1 km apart to avoid discrepancies resulting from spatial inhomogeneities.

Although the accelerometer-based DWR Mk-II buoys performed well in the mild conditions experienced during the 2009 experiment, these larger buoys could be deployed safely only on a few occasions in the higher-energy 2010 experiment. Furthermore, since these buoys were not equipped with internal dataloggers, the 2010 data were degraded by intermittent dropouts in the telemetry system. Therefore, only the 2009 data were used for these buoys.

The GPS-based DWR-G buoys were equipped with internal dataloggers that recorded displacement time series continuously. In high wind conditions, the GPS data contain occasional dropouts that may be caused by submergence of the antenna in breaking waves. The maximum data loss, experienced in the most energetic sea states, was about 0.5%. Most of these dropouts were isolated missing data points that were readily corrected through interpolation using the gap repair software provided by Datawell. On a few occasions, longer (5–10 s) continuous dropouts in the GPS signal occurred that could not be repaired, and these data were excluded from the analysis.

The absolute position data collected with various GPS position receivers (the Magellan, Locosys, and GlobalSat systems) did not contain dropouts or other visually obvious data glitches, and were used here in their raw form.

b. Time series

The internal buoy processing of the Datawell displacement time series includes a high-pass filter to remove low-frequency motions. The cutoff frequency is 0.033 Hz for the

DWR Mk-II buoys and 0.01 Hz for the DWR-G buoys. The GPS position receivers record absolute buoy position. To remove the buoy drift and low-frequency variability, a simple high-pass filter in the time domain was applied to the north, west, and altitude time series by subtracting a 60-s moving average. The slightly different cutoff frequencies used for different instruments do not have a significant effect on the filtered wave time series because the variance in the 20–200-s infra-gravity range is about two orders of magnitude lower than the wind-sea and swell variance.

To allow for detailed comparisons of different sensors on the same buoy an accurate time base is needed. All the GPS position receivers record GPS time marks with the position data every second. Hence, the GPS receiver time series keep accurate time both in an absolute sense and relative to each other. The timing of the Datawell buoy data stream, sampled at a slightly faster rate of 1.28 Hz, is controlled by an autonomous computer clock, which is inherently less accurate than the GPS time base. Additionally, the buoy data collection is affected by miscellaneous filters that cause time delays of about 5 min. To precisely synchronize the Datawell and GPS receiver time series on a common UTC time base, a cross-correlation analysis was performed on the east–west displacements measured by the Datawell sensor and one of the GPS position receivers on the same buoy. Since the horizontal wave orbital displacements are accurately resolved by all GPS receivers used in this study (see next section), the time delay between the Datawell and GPS receiver records can be determined unambiguously from the maximum of the cross-correlation function. The Datawell time series (north, west, and vertical displacements) were shifted by the estimated time difference and interpolated onto the time marks of the GPS receiver to obtain time series with a common time base and the same 1-Hz sample rate.

c. Spectral analysis

The processed 8192-s-long data records of Datawell buoys and GPS receivers sample vertical (z) and horizontal (x, y) buoy displacements every second. Since the buoy drift is typically small (i.e., less than 10%) compared to the dominant surface wave speeds, these time series $x(t)$, $y(t)$, $z(t)$ describe (to leading order in wave steepness) the wave orbital motion at a fixed location. Conventional auto- and cross-spectral analysis was applied to the time series using overlapping 1024-s-long segments and a Hamming window. Merging seven frequency bands yields a smoothed set of spectra, including autospectra $E_{xx}(f)$, $E_{yy}(f)$, $E_{zz}(f)$, the cospectrum of the horizontal displacements $C_{xy}(f)$, and quadrature-spectra of horizontal and vertical displacements $Q_{xz}(f)$, $Q_{yz}(f)$, all with a frequency resolution of 0.0068 Hz and approximately 112 degrees of freedom. The remaining

co- and quadrature-spectra $Q_{xy}(f)$, $C_{xz}(f)$, $C_{yz}(f)$ vanish for linear surface gravity waves and are not considered here.

The analysis was restricted to the frequency range $0.05 \text{ Hz} < f < 0.3 \text{ Hz}$ that contains the dominant wind-sea and swell waves. For a typical developed wind-sea state with a peak frequency of 0.1 Hz this range extends to about 3 times the peak frequency where possibly significant tertiary nonlinear contributions to the wave field complicate the interpretation of measurements. Lower-frequency ($< 0.05 \text{ Hz}$), so-called infra-gravity waves are not considered here because the internal high-pass filters in the Datawell buoys effectively remove these signals from the data stream.

The vertical displacement spectrum $E_{zz}(f)$ yields a direct estimate of the wave frequency spectrum $E(f)$. In the deep-water limit (which is a reasonable approximation for all the data presented here) the linear wave orbital motion is circular and thus $E_{xx}(f) + E_{yy}(f) = E_{zz}(f) = E(f)$. Srokosz and Longuet-Higgins (1986) show theoretically that the Lagrangian displacements of a surface-following buoy in deep water exactly cancel out the high-frequency second-order bound waves so that the characteristic steepening of wave crests and broadening of troughs is not observed in a buoy record. Therefore, the equality of horizontal and vertical buoy displacement spectra may be expected to hold even in higher-sea states with a significant second harmonic contribution to the Eulerian surface elevation spectrum. The sum of the horizontal displacement spectra provides an alternative, and potentially more accurate, estimate of the wave frequency spectrum, because horizontal positions are generally more accurately measured by GPS receivers than vertical elevation.¹

A representative wave height and period are readily estimated from the wave frequency spectrum. Here the common definition of significant wave height $H_s \equiv 4E^{1/2}$ is used with $E = \int_{0.05 \text{ Hz}}^{0.3 \text{ Hz}} E(f) df$ the surface elevation variance in the swell-sea frequency range. The mean wave period is estimated in a similar fashion based on an energy-weighted mean wave frequency, $T_m = E / \int_{0.05 \text{ Hz}}^{0.3 \text{ Hz}} f E(f) df$. These bulk parameters were estimated based on both the vertical and horizontal displacement spectra to assess the effects of differences between vertical and horizontal GPS position accuracy.

d. Directional analysis

The Datawell buoys and GPS position receivers all provide displacement time series $x(t)$, $y(t)$, $z(t)$ that can be

¹ This approach is readily extended to finite depth by applying the linear theory correction $\tanh^2(kh)[E_{xx}(f) + E_{yy}(f)] = E(f)$ with k the wavenumber given by the linear dispersion relation and h the water depth.

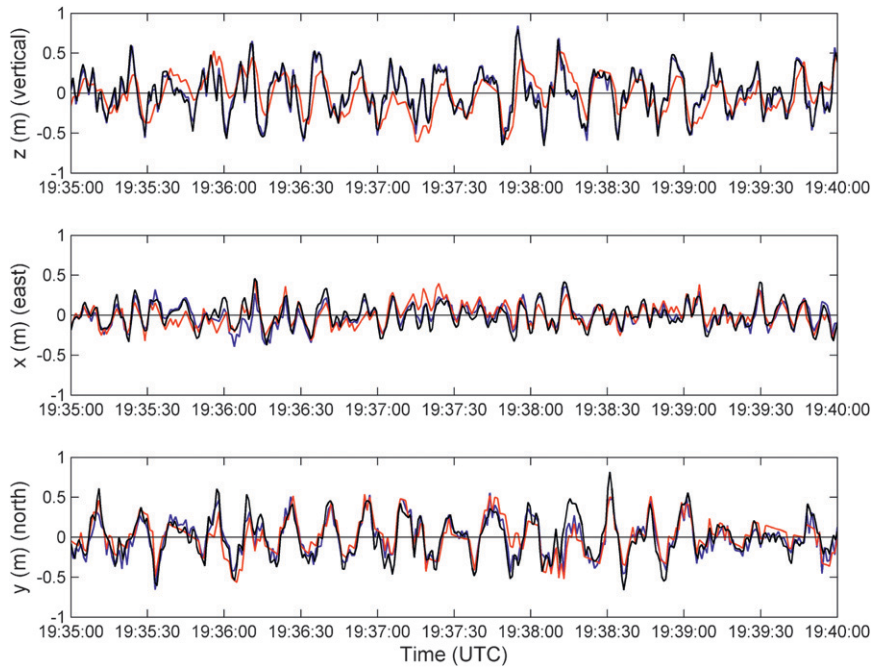


FIG. 2. Example comparison of wave orbital displacement time series measured by three sensors on the same drifting buoy. The observations were taken on 3 Jun 2009 in benign swell conditions. (top to bottom) Vertical, east, and north displacements. Measurements obtained with the internal buoy motion package (accelerometer-tilt-compass sensors) are indicated in black; GPS position receiver data are in blue (Magellan) and red (Locosys).

analyzed with standard methods (e.g., Kuik et al. 1988 and references therein) to estimate the mean wave direction $\bar{\theta}$ and directional spread σ_θ as functions of frequency. Here the direction θ is defined in a coordinate system with the x axis pointing east and the y axis pointing north ($\theta = 0$ for waves traveling to the east, 90° to the north). The lowest four Fourier moments of the directional distribution of wave energy $S(\theta)$ at each frequency can be expressed in terms of normalized cross spectra (Long 1980):

$$\begin{pmatrix} a_1 \\ b_1 \\ a_2 \\ b_2 \end{pmatrix} \equiv \int_0^{2\pi} \begin{pmatrix} \cos\theta \\ \sin\theta \\ \cos 2\theta \\ \sin 2\theta \end{pmatrix} S(\theta) d\theta, \tag{1}$$

$$= \begin{bmatrix} Q_{xz}/\sqrt{(E_{xx} + E_{yy})E_{zz}} \\ Q_{yz}/\sqrt{(E_{xx} + E_{yy})E_{zz}} \\ (E_{xx} - E_{yy})/(E_{xx} + E_{yy}) \\ 2C_{xy}/(E_{xx} + E_{yy}) \end{bmatrix}.$$

The most widely used estimates of $\bar{\theta}$ and σ_θ are based on the first-order moments:

$$\tan(\bar{\theta}) \equiv b_1/a_1, \tag{2a}$$

$$\sigma_\theta \equiv \sqrt{2\left(1 - \sqrt{a_1^2 + b_1^2}\right)}, \tag{2b}$$

where $\bar{\theta}$, defined on a full circle, corresponds to the direction of the energy flux vector and σ_θ can be interpreted (in the limit of a narrow directional spectrum) as the standard deviation of $S(\theta)$.

Alternatively, estimates of $\bar{\theta}$ and σ_θ can be obtained from the second-order moments:

$$\tan(2\bar{\theta}) \equiv b_2/a_2, \tag{3a}$$

$$\sigma_\theta \equiv \sqrt{\left(1 - \sqrt{a_2^2 + b_2^2}\right)}/2, \tag{3b}$$

where $\bar{\theta}$, defined on a half circle, corresponds to the major axis of the horizontal wave orbital displacements and σ_θ describes the associated polarization (e.g., Herbers et al. 1999). Unlike (2a), $\bar{\theta}$ given by (3a) suffers from an 180° ambiguity. This can be an important drawback in open-ocean conditions where wave directions are not constrained by the presence of a shoreline. Both σ_θ estimates in (2b) and (3b) approximate the standard deviation of the directional distribution of wave energy, with a negative

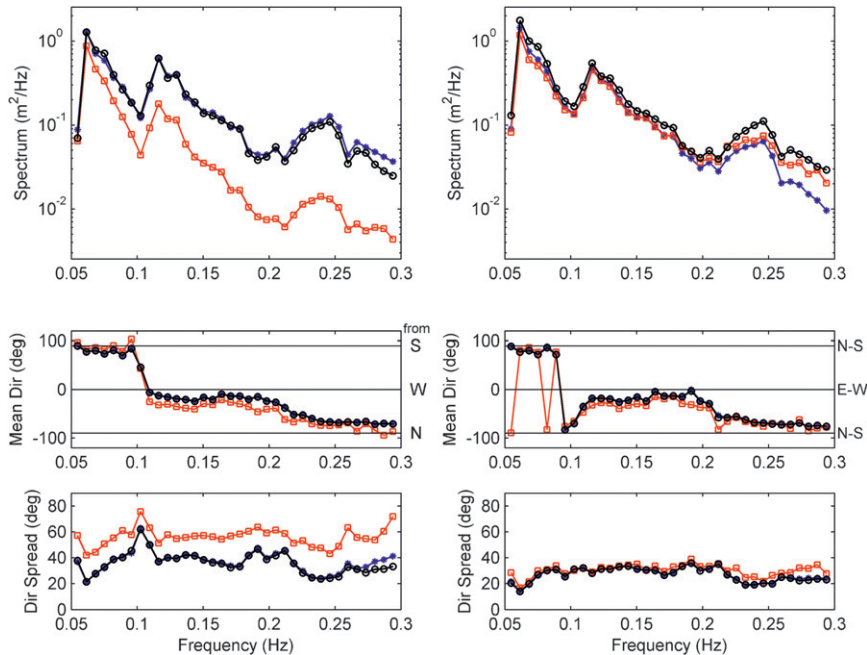


FIG. 3. Comparison of wave spectra estimates from three sensors on the same drifting buoy deployed on 3 Jun 2009. (top to bottom) Wave frequency spectra $E(f)$, frequency-dependent mean direction $\bar{\theta}(f)$, and directional spread $\sigma_{\theta}(f)$. (left) Estimates based on vertical elevation measurements and first-order directional moments [Eqs. (2a) and (2b)]. (right) Estimates based on horizontal displacement measurements and second-order directional moments [Eqs. (3a) and (3b)]. Estimates obtained with the internal buoy motion package are displayed in black lines with circles; GPS-based estimates are displayed in blue lines with asterisks (Magellan) and red lines with squares (Locosys).

bias that increases with directional spreading. This bias is larger for (3b) than (2b), and the estimates can differ substantially for broad spectra [e.g., the maximum σ_{θ} values for an isotropic spectrum are $\sqrt{2}(81^{\circ})$ for (2b) and $1/\sqrt{2}(40.5^{\circ})$ for (3b)] (see Herbers et al. 1999 for a more thorough discussion).

Although estimates of $\bar{\theta}$ and σ_{θ} based on the first-order moments in (2a) and (2b) are perhaps more straightforward to interpret, they depend on measurements of both horizontal and vertical displacements. The second-order moment in (3a) and (3b) depends only on horizontal displacements, and thus may be more accurate for some GPS systems with degraded vertical accuracy. In this study, estimates based on both (2a), (2b) and (3a),(3b) are evaluated to assess their accuracy for different buoys and sensors.

In addition to frequency-dependent estimates $\bar{\theta}(f)$ and $\sigma_{\theta}(f)$, energy-weighted bulk estimates were obtained by integrating the auto- and cross spectra in Eq. (1) over the swell-sea frequency range.

4. Sensor intercomparisons

Three different types of sensor systems were used to measure waves in this study. The Datawell DWR Mk-II

buoys are equipped with accelerometers–tilt–compass sensors (ATC) whereas the sensor package in the DWR-G7 and DWR-G4 buoys is based on the Doppler shift in GPS signals (GDOP). The wave measurements from the Magellan, Locosys, and GlobalSat GPS receivers are all based on SBAS absolute position data (GPOS). The ATC system is an autonomous motion package and thus yields wave measurements that are completely independent from those provided by the satellite-based GDOP and GPOS sensors. Here measurements are compared obtained with these different types of sensor systems mounted on the same buoy.

a. GPS position receivers and Datawell accelerometer buoys

ATC and GPOS measurements of long-period swell ($H_s = 0.9$ m) observed on 3 June 2009 are compared in Figs. 2 and 3. The Magellan and Locosys GPOS sensors were both mounted on the same Datawell DWR Mk-II buoy that contains the ATC sensor. An example comparison of 5-min-long vertical and horizontal displacement time series is shown in Fig. 2. The vertical (top panel) and north–south (bottom panel) displacements are dominated by a southerly swell, while a weaker

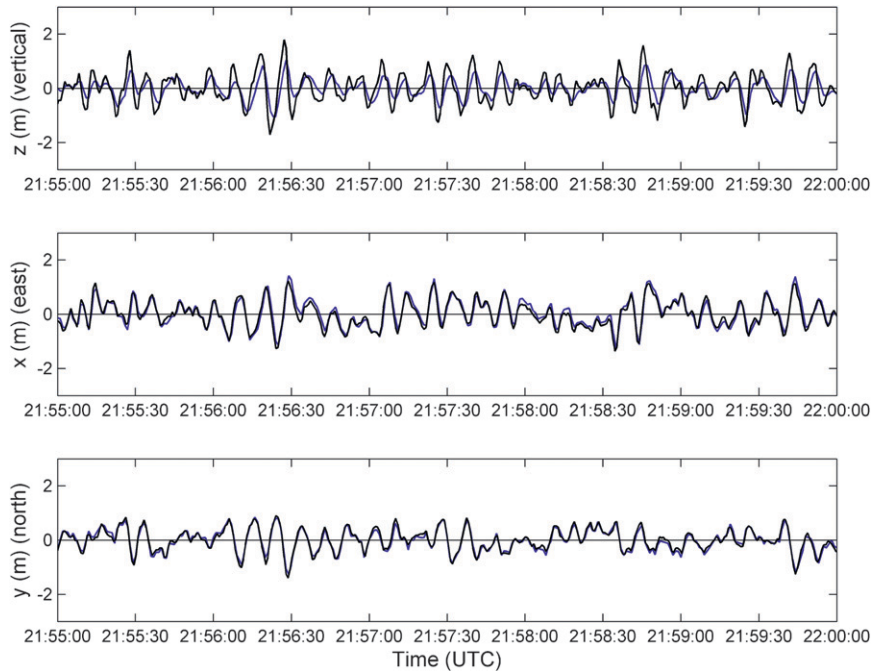


FIG. 4. Example comparison of wave orbital displacement time series measured by a Datawell DWR-G4 buoy and a Locosys GPS position receiver mounted on the same buoy. The observations were taken on 21 Jun 2010 in moderately energetic wind-sea conditions. (top to bottom) Vertical, east, and north displacements. Measurements obtained with the internal buoy sensor (based on the Doppler shift in GPS signals) are indicated in black; GPS position receiver data are in blue.

higher-frequency wave system is observed in the east–west (middle panel) displacements. The agreement between the Magellan GPOS sensor and the ATC sensor is excellent for both vertical and horizontal displacements (cf. the blue and black curves). The Locosys GPOS measurements also agree well with the ATC records of horizontal displacements. However, significant errors are apparent in the vertical displacements (cf. the red and black curves). The waves are resolved in the GPOS record, but with strongly reduced amplitudes suggesting possible contamination of the vertical position data by multipath reflections of the GPS signal.

The spectral wave statistics obtained from the three sensors for the entire 137-min-long data record are compared in Fig. 3. Shown in the left panels are traditional estimates of the wave frequency spectrum $E(f)$, and the mean wave direction $\bar{\theta}(f)$ and directional spread $\sigma_{\theta}(f)$ (as functions of frequency) based on the vertical displacement spectrum and first-order directional moments [Eqs. (2a) and (2b)]. The agreement between the Magellan GPOS sensor (blue asterisks) and the ATC sensor (black circles) is excellent across the entire spectrum with three distinct peaks. The Locosys GPOS estimates (red squares) on the other hand show greatly

reduced spectral levels and enhanced directional spreading owing to the low quality of the vertical displacement measurements.

Alternative estimates of the same spectral wave statistics based on horizontal displacement spectra and second-order directional moments [Eqs. (3a) and (3b)] are compared in the right panels of Fig. 3. These estimates use only horizontal displacement data and thus are not affected by the low quality of the Locosys vertical position data. Indeed, the agreement with the ATC estimates is excellent, confirming that useful routine wave information can be obtained from this inexpensive sensor. The Magellan GPOS yields comparably good agreement with the ATC estimates for both the vertical/first-order and horizontal/second-order analysis, suggesting that this GPS position sensor has the full capabilities of a heave–pitch–roll wave measurement system.

b. GPS position receivers and Datawell GPS buoys

Locosys GPS receivers were mounted on the Datawell DWR-G4 Mini Directional Waverider buoys during most deployments to allow for intercomparisons of the Locosys GPOS and Datawell GDOP measurements. A case example for a moderately energetic wind sea ($H_s = 2.0$ m)

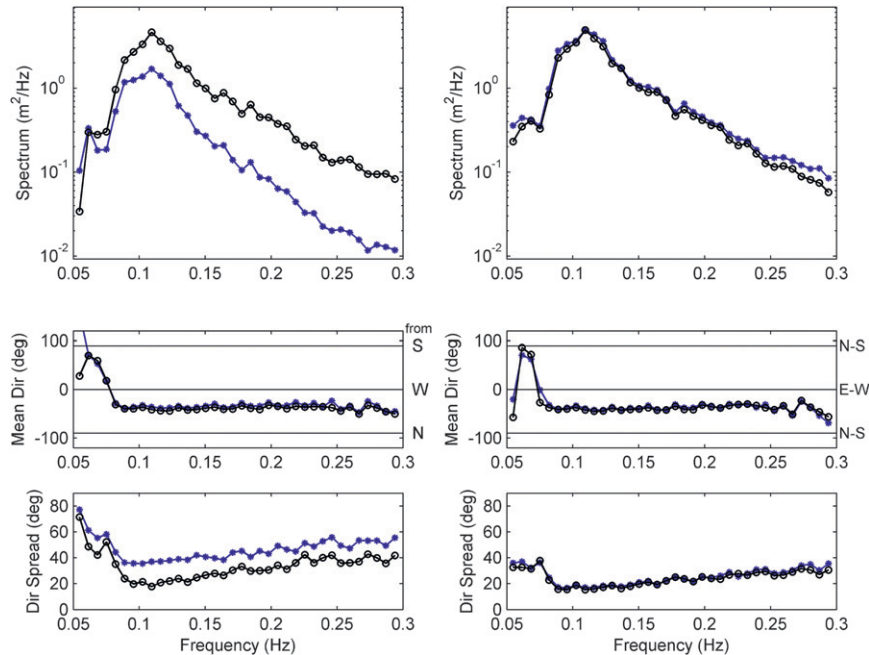


FIG. 5. Comparison of (top to bottom) wave energy and direction spectra observed on 21 Jun 2010 with a drifting Datawell DWR-G4 buoy (black lines with circles) and a Locosys GPS position receiver mounted on the same buoy (blue lines with asterisks). (left) Estimates based on vertical elevation measurements and first-order directional moments [Eqs. (2a) and (2b)]. (right) Estimates based on horizontal displacement measurements and second-order directional moments [Eqs. (3a) and (3b)].

observed on 21 June is detailed in Figs. 4 and 5. The time series of horizontal displacements (middle and bottom panel of Fig. 4) show excellent agreement between the GPOS (blue) and GDOP (black) measurements. On the other hand the agreement is poor for vertical displacements (top panel) where the GPOS measurements record wave fluctuations that are coherent with the GDOP measurements, but about a factor of 2 smaller. This notable difference in the vertical and horizontal accuracy is also reflected in the wave frequency and directional spectra shown in Fig. 5. The GPOS estimate of $E(f)$ based on vertical displacements is about a factor of 5 lower than the GDOP estimate at the spectral peak and almost an order of magnitude lower at higher frequencies (top-left panel). Significant discrepancies are also noted in the corresponding [i.e., based on first-order moments in Eqs. (2a) and (2b)] $\sigma_\theta(f)$ estimates (bottom-left panel). However, the $\bar{\theta}(f)$ estimates are in good agreement (middle-left panel), indicating that the vertical displacements measured with the GPS receiver, although attenuated, do accurately resolve the wave phase relations.

Alternative estimates of $E(f)$, $\bar{\theta}(f)$, and $\sigma_\theta(f)$, based entirely on horizontal displacement measurements, show excellent agreement between the Locosys GPOS and Datawell GDOP sensors (Fig. 5, right panels). A high level

of agreement in wave spectra estimates based on horizontal displacement measurements was observed in all the 2010 cases with moderate–high-energy wind-sea conditions. The somewhat improved performance relative to the lower-energy swell conditions of 2009 (Fig. 3, right panels) may reflect a higher signal-to-noise ratio.

Finally, estimates of $E(f)$, $\bar{\theta}(f)$, and $\sigma_\theta(f)$, obtained from a GlobalSat GPOS sensor mounted on the moored Datawell DWR-G7 buoy, are compared with estimates from the Datawell GDOP sensor on the same buoy in Fig. 6. The observations were taken on 14 June when the significant wave height reached a maximum value of 4.0 m. The results are generally similar to those for the Locosys sensor (Figs. 4 and 5) with excellent agreement for estimates of $E(f)$, $\bar{\theta}(f)$, and $\sigma_\theta(f)$ based on horizontal displacement measurements (right panels) and poor agreement if vertical displacement measurements are used (left panels).

c. Summary statistics of bulk wave parameters

To summarize the sensor performance for all buoy deployments (Table 2), comparisons of estimates of bulk wave parameters are shown in Figs. 7 and 8. Estimates of the significant wave height H_s , the mean wave period T_m , the mean direction $\bar{\theta}$, and directional spread σ_θ obtained

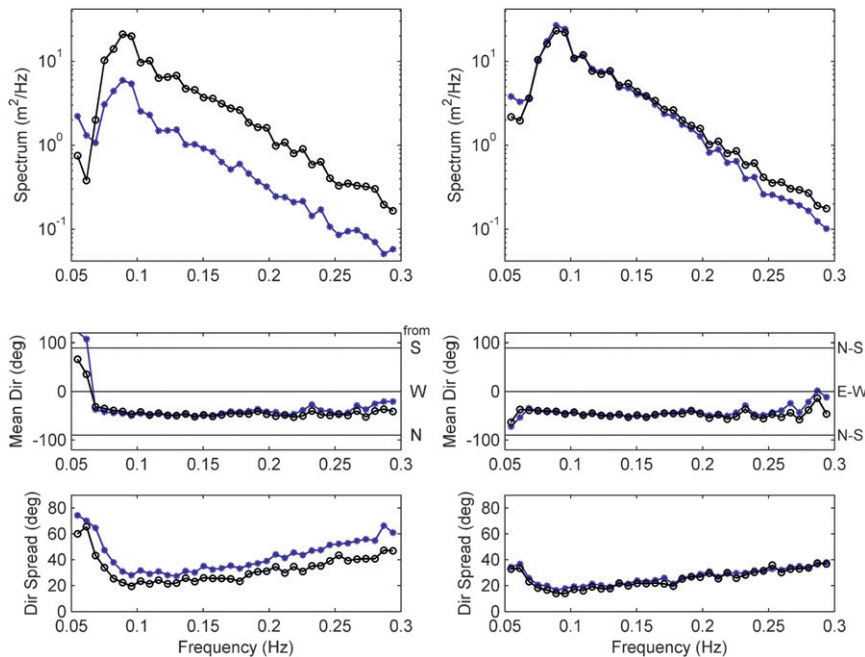


FIG. 6. As in Fig. 5, but observed during the most energetic wave event on 14 Jun 2010 with a moored Datawell DWR-G7 buoy (black lines with circles) and a GlobalSat GPS position receiver mounted on the same buoy (blue lines with asterisks).

from GPS position receivers (GPOS) are compared in scatter diagrams with estimates from the Datawell sensor (ATC or GDOP) on the same buoy. Traditional estimates based on vertical displacement spectra and first-order directional moments are presented in Fig. 7. Alternative estimates based on horizontal displacement spectra and second-order directional moments are presented in Fig. 8. The latter estimates do not use vertical displacement measurements and thus are expected to be more robust for GPS receivers with poor vertical accuracy.

As expected from the previous discussion of case study examples, the H_s estimates obtained from vertical GPS position data are biased low compared with the Datawell estimates (Fig. 7, top left), with the exception of the Magellan system that was equipped with a precision antenna (blue dots). The relative bias for the Locosys (green dots) and GlobalSat (red dots) estimates varies significantly between different deployments, suggesting there is no simple empirical transfer function correction to remove the bias. Similar errors are noted for the Locosys and GlobalSat sensors in the other bulk parameters, with considerable scatter and a high bias in the period T_m (top-right panel) and directional spread σ_θ (bottom right), but reasonably good agreement for the mean direction $\bar{\theta}$ (bottom left).

The alternative estimates based on horizontal displacement measurements show a dramatic improvement

for all bulk parameters, with typical errors of only a few percent for H_s and T_m , a few degrees for $\bar{\theta}$, and less than 10% for σ_θ . The $\bar{\theta}$ estimates based on second-order moments [Eq. (3a)] suffer from a 180° ambiguity, but the half-plane of wave propagation may be resolved by combining them with the noisier (but unambiguous) estimates based on first-order moments [Eq. (2a) and Fig. 7]. Overall, these comparisons show that reliable routine wave information can be extracted from inexpensive off-the-shelf GPS receivers.

5. Buoy and drifter comparisons

The intercomparisons of wave measurements obtained with different sensors on the same buoy generally show consistent results for sensors using accelerometers, GPS Doppler data, and GPS position data. However, the data quality may be affected not only by the sensor performance, but also by the wave-following properties of the buoy. Here wave measurements from buoys with different sizes and shapes, drifting in close proximity to each other are compared, to evaluate the combined effect of sensor and buoy response characteristics on wave-measuring capabilities. The buoys include Datawell Waverider buoys with spherical hulls in three different sizes (0.9-, 07-, and 0.4-m diameter) and a prototype buoy similar in size to the smallest Datawell buoy, but with cylindrical flotation

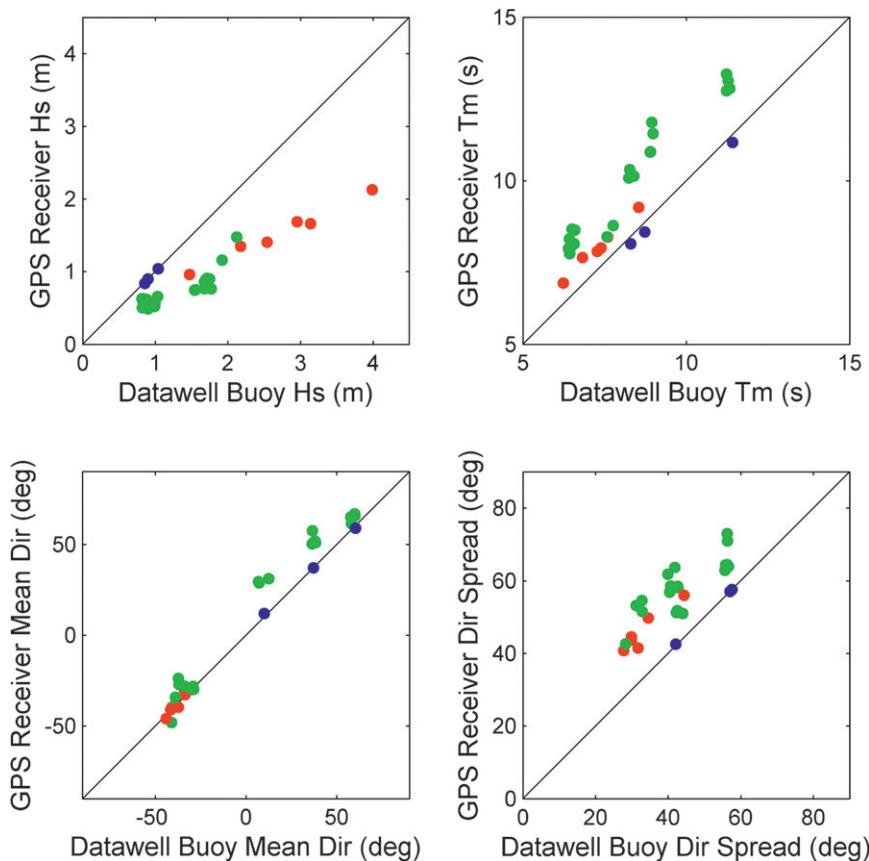


FIG. 7. Bulk wave parameter estimates based on vertical elevation measurements and first-order directional moments [Eqs. (2a) and (2b)]. Estimates from GPS position receivers are shown in scatter diagrams vs estimates from the Datawell sensor on the same buoy. Blue discs: Magellan GPS receiver on drifting Mk-II buoy. Green discs: Locosys GPS receiver on drifting DWR-G4 or DWR-G7 buoy. Red discs: GlobalSat GPS receiver on moored DWR-G7 buoy.

elements (Fig. 1). In these drifting deployments of a cluster of buoys, the buoy separations remained within 1 km, and over these relatively short distances [$O(5$ wavelengths)] the wave field is expected to be homogeneous in a statistical sense. Estimates of wave frequency spectra $E(f)$, and frequency-dependent mean direction $\bar{\theta}(f)$, and directional spread $\sigma_{\theta}(f)$ [obtained with the standard method using vertical elevation measurements and first-order directional moments in Eqs. (2a) and (2b)] are compared in swell-dominated (2009 experiment) and wind-sea-dominated (2010) conditions.

Results for 3 June 2009 with benign swell conditions ($H_s = 0.9$ m) are shown in Fig. 9. In this deployment, five Datawell buoys were deployed including one DWR Mk-II (0.9-m diameter, black curves), two DWR-G7 (0.7 m, green), and two DWR-G4 (0.4 m, blue). Deployed in a tight cluster, the buoys drifted north with a surface current of about 0.25 m s^{-1} . While the smaller (0.4- and 0.7-m diameter) buoys stayed close together, the larger

(0.9 m) buoy drifted farther east suggesting some possibly windage effect from the packages mounted on the buoy. Estimates of the wave energy and direction spectra $E(f)$, $\bar{\theta}(f)$, and $\sigma_{\theta}(f)$ are all in good agreement, resolving a complex trimodal wave field with a dominant narrow-band 0.06-Hz swell from the Southern Hemisphere, an intermediate wave system with a peak frequency of 0.14 Hz arriving from a westerly direction, and a weak high-frequency (about 0.25 Hz) wind sea from the north.

Comparisons for more energetic wave conditions in the 2010 experiment are detailed in Fig. 10. Results are shown for four occasions when the new prototype GPS drifters were deployed together with DWR-G7 and DWR-G4 buoys. The observations of moderately energetic sea states ($H_s = 1.7\text{--}2.1$ m) include narrow- and broadband wave spectra with both uni- and bimodal shapes. In all four cases, the dominant waves are driven by the prevailing strong winds from the north-west, with a variable lower-frequency Southern Hemisphere swell

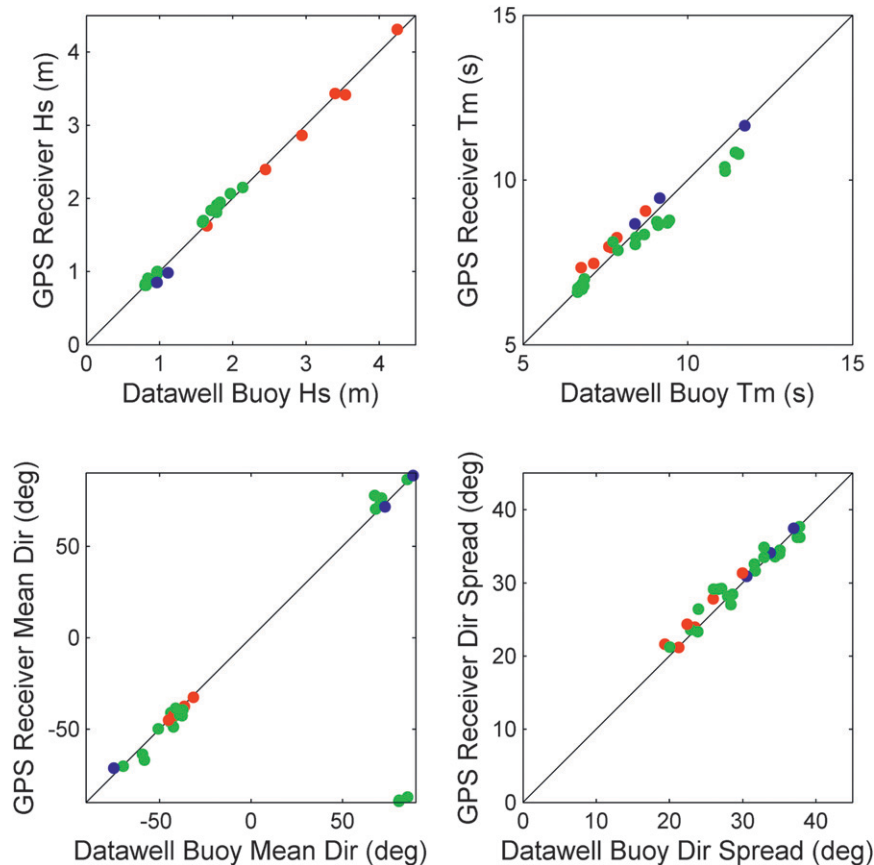


FIG. 8. Bulk wave parameter estimates based on horizontal displacement measurements and second-order directional moments [Eqs. (3a) and (3b)]. Estimates from GPS position receivers are shown in scatter diagrams vs estimates from the Datawell sensor on the same buoy. Format as in Fig. 7.

contribution. Estimates of the wave energy and direction spectra $E(f)$, $\bar{\theta}(f)$, and $\sigma_{\theta}(f)$ obtained with the prototype GPS drifters (red curves) are generally in good agreement with the Datawell buoys (green and blue curves), with the exception of the high-frequency spectral tail where the higher spectral levels and directional spreading values suggest higher noise levels as noted also in the intercomparisons of sensors on the same buoy (section 4). Similarly, the higher spectral levels below the spectral peak recorded by the prototype drifter on 12 June (top-left panel) are indicative of measurement errors. Overall, the consistently good agreement demonstrates that these relatively inexpensive drifters using off-the-shelf GPS receivers can resolve the detailed spectral properties of ocean surface waves.

6. Summary and conclusions

Recent developments in global positioning system (GPS) technology have enabled in situ ocean wave measurements at a relatively low cost with surface-following buoys. Compared with traditional heave-pitch-roll

buoys that use an autonomous motion package with accelerometers-tilt-compass sensors, GPS buoys are considerably less expensive, have no moving parts, do not require calibration, and can accommodate a compact hull size for easy deployment from a small boat. In this study a field evaluation of GPS buoys is presented to assess their accuracy and robustness for routine wave measurements.

Field experiments were conducted in deep water off the California coast to collect GPS buoy measurements in a range of open-ocean wind-sea and swell conditions. The buoys included Datawell DWR-G Waveriders equipped with a specialized GPS sensor package that measures the buoy displacements based on the Doppler shift in GPS signals, as well as the older (and well established) Datawell Mk-II buoys with an accelerometer-tilt-compass sensor package. The wave-resolving capabilities of several inexpensive off-the-shelf GPS position receivers (Magellan, Locosys, and GlobalSat) were evaluated by mounting them externally on the Datawell buoys and in a new prototype drifter.

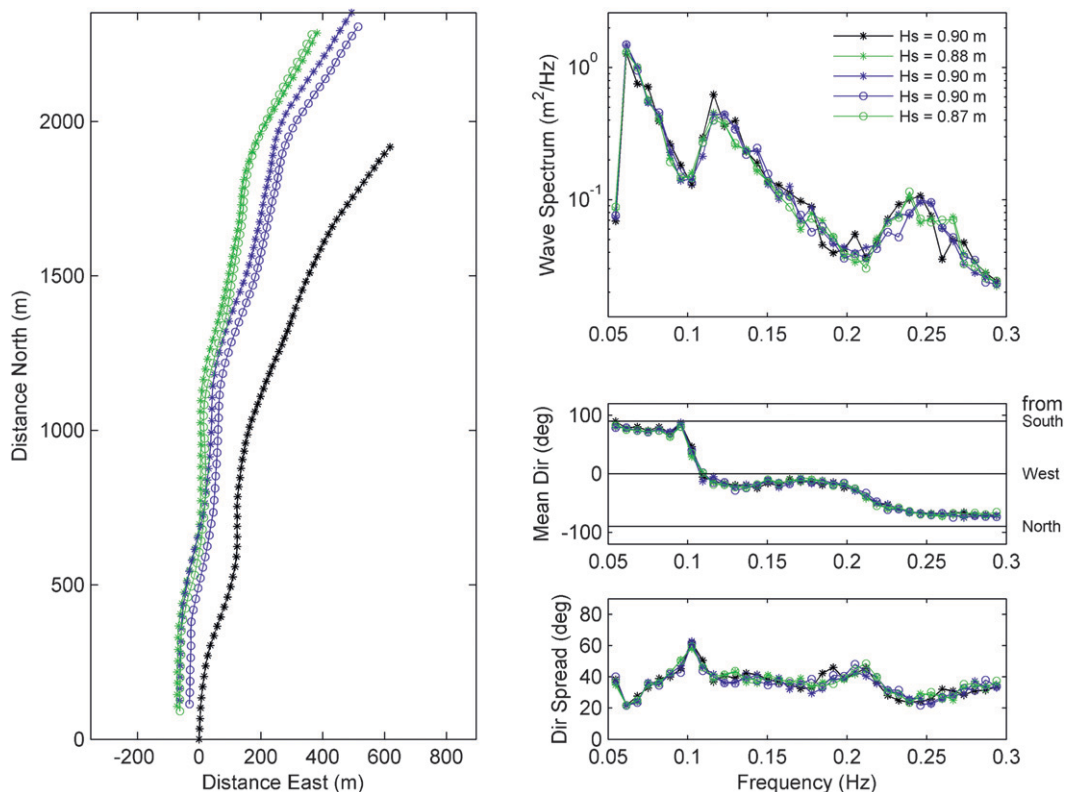


FIG. 9. Comparison of observations from five drifting Datawell buoys deployed on 3 Jun 2009. The buoys include one Mk-II (black curves), two DWR-G7 (green), and two DWR-G4 (blue) buoys. (left) Drift tracks with the origin corresponding to the initial position of the Mk-II buoy. (right, top to bottom) Wave frequency spectra $E(f)$, frequency-dependent mean direction $\bar{\theta}(f)$, and directional spread $\sigma_{\theta}(f)$. The estimates are based on vertical elevation measurements and first-order directional moments [Eqs. (2a) and (2b)].

Although the absolute position accuracy of the GPS receivers (using SBAS real-time differential corrections) is limited to a few meters, comparisons with the Datawell wave measurements (both GPS and accelerometer based) show surprisingly good agreement, even in benign swell conditions with wave orbital excursions less than 1 m. Horizontal wave orbital displacements are accurately resolved by all three GPS receivers. Vertical displacement fluctuations are accurately measured by the Magellan receiver equipped with a precision external antenna, but significantly damped in the data from the other GPS receivers, suggesting the internal (Locosys) and small patch (GlobalSat) antennas suffer from multipath reflections.

Wave measurements from different Datawell buoys (0.9-m diameter accelerometer and 0.7- and 0.4-m GPS) and prototype drifters (0.45-m diameter with Magellan GPS receiver) were compared in several deployments where the buoys were drifting in close proximity to each other. Spectral estimates of wave energy, mean direction, and directional spread are generally in good agreement. Compared with the Datawell buoys, the prototype buoys show somewhat elevated energy levels and directional

spreading values at high frequencies, suggesting higher noise levels. The Datawell GPS buoys occasionally suffer from GPS signal dropouts in high sea states. Overall the comparisons demonstrate that all these buoys can provide detailed wave information across the wind-sea and swell frequency bands.

Although off-the-shelf GPS position receivers may not always yield the high data quality of Datawell Waverider buoys, the results of this study demonstrate that they can provide accurate and useful routine wave information, and at a fraction of the cost. Even small and inexpensive hand-held GPS receivers are shown to accurately resolve wave-induced horizontal displacements, from which estimates of standard wave statistics (e.g., wave energy and mean direction spectra, and bulk wave parameters) can be obtained. While the quality of the spectral data is high, the directional information is limited by the 180° direction ambiguity of the horizontal displacement data. This may limit the usefulness of off-the-shelf GPS receivers with poor vertical accuracy for routine wave monitoring applications, especially in open-ocean conditions where waves can arrive from all directions. In

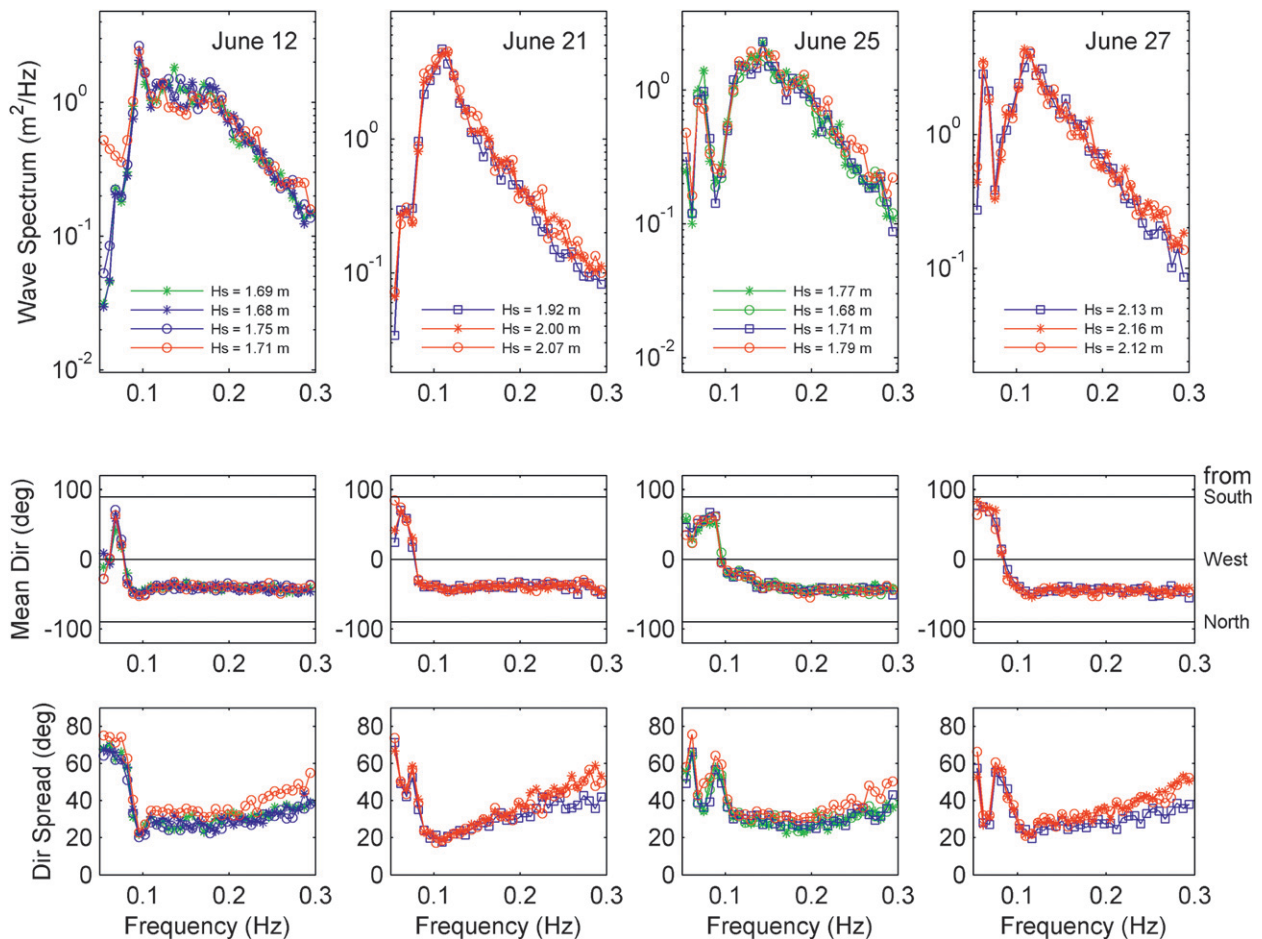


FIG. 10. Comparison of wave observations from Datawell DWR-G7 (green curves) and DWR-G4 (blue) buoys, and prototype GPS drifters (red), drifting within 1 km from each other. (left to right) Results from four deployments in June 2010. (top to bottom) Wave frequency spectra $E(f)$, frequency-dependent mean direction $\bar{\theta}(f)$, and directional spread $\sigma_{\theta}(f)$. The estimates are based on vertical elevation measurements and first-order directional moments [Eqs. (2a) and (2b)].

complex sea states the horizontal GPS drift tracks are clearly insufficient, and full three-axis displacement measurements or a multicomponent array may be required to resolve crossing waves at the same frequency. Additionally GPS drifters may get submerged in large breaking waves causing data gaps that may limit their usefulness for monitoring extreme wave occurrences.

GPS position receivers are already widely used in drifters to measure open-ocean and coastal currents. This study shows that these inexpensive sensors are also accurate in the surface-wave frequency band, a capability that could be exploited to develop a low-cost GPS drifter for collecting both wave and current observations. In the open ocean, wave data are usually derived from satellite altimeter measurements that yield accurate significant wave height estimates with excellent spatial coverage, but do not provide spectral wave information. A network of open-ocean GPS drifters can provide accurate estimates of wave

frequency spectra that could prove valuable in the validation and improvement of basin-scale wind-wave prediction models.

Acknowledgments. This research is supported by the Office of Naval Research (Physical Oceanography Program and Littoral Geosciences and Optics Program). The captain and crew of the R/V *Gordon Sproul* provided excellent support in the field experiments. Helpful suggestions by the anonymous reviewers are very much appreciated.

REFERENCES

- Allender, J., and Coauthors, 1989: The WADIC project: A comprehensive field evaluation of directional wave instrumentation. *Ocean Eng.*, **16** (5–6), 505–536.
- Ancil, F., M. A. Donelan, G. Z. Forristall, K. E. Steele, and Y. Ouellet, 1993: Deep-water field evaluation of the NDBC-SWADE 3-m discus directional buoy. *J. Atmos. Oceanic Technol.*, **10**, 97–112.

- Barstow, S. F., G. Ueland, H. E. Krogstad, and B. A. Fossum, 1991: The Wavescan second generation directional wave buoy. *IEEE J. Oceanic Eng.*, **16** (3), 254–266.
- de Vries, J. J., J. Waldron, and V. Cunningham, 2003: Field tests of the new Datawell DWR-G GPS wave buoy. *Sea Technol.*, **44**, 50–55. [Available online at http://download.datawell.nl/documentation/datawell_publication_dwr-g_seatechnology-dec2003_2003-12-01.pdf.]
- George, R., and J. L. Largier, 1996: Description and performance of finescale drifters for coastal and estuarine studies. *J. Atmos. Oceanic Technol.*, **13**, 1322–1326.
- Hauser, D., K. Kahma, H. E. Krogstad, S. Lehner, J. A. J. Monbaliu, and L. R. Wyatt, Eds., 2005: Measuring and analyzing the directional spectra of ocean waves. Office for Official Publications of the European Communities, EUR 21367 COST Action 714, Luxembourg, 465 pp.
- Herbers, T. H. C., S. Elgar, and R. T. Guza, 1999: Directional spreading of waves in the nearshore. *J. Geophys. Res.*, **104** (C4), 7683–7693.
- Johnson, D., R. Stocker, R. Head, J. Imberger, and C. Pattiaratchi, 2003: A compact, low-cost GPS drifter for use in the oceanic nearshore zone, lakes, and estuaries. *J. Atmos. Oceanic Technol.*, **20**, 1880–1884.
- Krogstad, H. E., S. F. Barstow, S. E. Aasen, and I. Rodriguez, 1999: Some recent developments in wave buoy measurement technology. *Coastal Eng.*, **37** (3–4), 309–329.
- Kuik, A. J., G. P. van Vledder, and L. H. Holthuijsen, 1988: A method for routine analysis of pitch-and-roll buoy data. *J. Phys. Oceanogr.*, **18**, 1020–1034.
- Long, R. B., 1980: The statistical evaluation of directional spectrum estimates derived from pitch/roll buoy data. *J. Phys. Oceanogr.*, **10**, 944–952.
- Longuet-Higgins, M. S., D. E. Cartwright, and N. D. Smith, 1963: Observations of the directional spectrum of sea waves using the motions of a floating buoy. *Ocean Wave Spectra*, Prentice-Hall, 111–136.
- MacMahan, J., J. Brown, and E. Thornton, 2009: Low-cost handheld Global Positioning System for measuring surf-zone currents. *J. Coastal Res.*, **25** (3), 744–754.
- Mitsuyasu, H., F. Tasai, T. Suhara, S. Mizuno, M. Ohkusu, T. Honda, and K. Rikiishi, 1975: Observations of the directional spectrum of ocean waves using a Cloverleaf Buoy. *J. Phys. Oceanogr.*, **5**, 750–760.
- O'Reilly, W. C., T. H. C. Herbers, R. J. Seymour, and R. T. Guza, 1996: A comparison of directional buoy and fixed platform measurements of Pacific swell. *J. Atmos. Oceanic Technol.*, **13**, 231–238.
- Schmidt, W. E., B. T. Woodward, K. S. Millikan, R. T. Guza, B. Raubenheimer, and S. Elgar, 2003: A GPS-tracked surf zone drifter. *J. Atmos. Oceanic Technol.*, **20**, 1069–1075.
- Srokosz, M. A., and M. S. Longuet-Higgins, 1986: On the skewness of sea-surface elevation. *J. Fluid Mech.*, **164**, 487–497.